

INVESTIGATION OF FAILURE PROCESSES IN SANDSTONE BY MEANS OF
HOLOGRAPHIC INTERFEROMETRY

UNTERSUCHUNG VON VERSAGENSVORGÄNGEN IN SANDSTEIN MITTELS
HOLOGRAPHISCHER INTERFEROMETRIE

INVESTIGATION PAR HOLOGRAPHIQUE DE PROCÉDES DE RUPTURE DANS
DU GRES

Gunter Krüger
Gottfried Sawade

Abstract

Different kinds of natural stone (Schilfsandstein, Grünsandstein, Stubensandstein) were investigated with the aim to characterize them by a fracture mechanical description. The mechanical parameters and properties were evaluated from deformation controlled 3-point-bending-tests on notched prismatic samples. Holographic interferometry in real-time-technique was applied for crack length determination. The samples showed crack formation and crack growth prior the maximum load.

The specimens, prepared in this way with cracks of a defined length as a result of the first loading were cemented by a stone strengthener. Further bending tests were made on the cemented specimen. A comparison of the results between the first and second loading allowed a description of the effect of cementation with respect to stress transfer over cracks.

Zusammenfassung

Zur Charakterisierung des Bruchverhaltens verschiedener Sandsteinarten (Schilfsandstein, Grünsandstein, Stubensandstein) wurden die bruchmechanischen Parameter und Kennlinien im 3-Punkt-Biegezugversuch bestimmt. Die Belastung erfolgte verformungsgesteuert bis in den abfallenden Ast. Die holographische Interferometrie in Echtzeittechnik wurde zur Rißvermessung und -beobachtung eingesetzt. Es konnte festgestellt werden, daß die untersuchten Sandsteine bereits vor Aufbringen der Höchstlast Rißbildung und stabiles Rißwachstum und somit nichlineares Bruchverhalten zeigen.

Die Probekörper, die auf diese Weise mit einem definierten Biegezugriß präpariert werden konnten, wurden anschließend mit Steinverfestiger (auf der Basis von Kieselsäure-Ethylester) behandelt und nach vollständiger Aushärtung einer weiteren Biegebeanspruchung unterzogen. Aus den Vergleich der

Last-Verformungskurven und des Rißwachstums bei der Erstbelastung und nach der Verfestigung, läßt sich die Wirkung des Steinverfestigers in Bezug auf die Spannungsübertragung über die Rißflächen beschreiben.

Résumé

Pour caractériser le comportement à la rupture de différents types de grés (Schilfsandstein, Grünsandstein, Stubensandstein) on a déterminé les paramètres et propriétés mécaniques par des essais de flexion à trois points sous déformations contrôllées. L'interférence holographique à technique de temps réel était appliquée pour la détermination de la longueur des fissures. Avant que la charge maximum soit appliquée des fissures apparaissent sur les éprouvettes et s'accroissent encore.

Les éprouvettes ainsi préparées avec des fissures d'une longueur déterminée en tant que résultat d'un premier chargement de flexion, sont consolidées par un durcisseur de pierre. D'autres essais sont réalisés sur l'éprouvette consolidée. La comparaison des résultats provenant du premier et second chargement a permis de décrire l'effet de consolidation en vue du transfert de tensions par les fissures.

Key words:

Schilfsandstein, Grünsandstein, Stubensandstein, Fracture Behaviour, Stone Strengthener, Real-time Holographic Interferometry,

1. Introduction

Mechanical and thermal-hygical loading of buildings made of natural stone can lead in conjunction with chemical and biological deterioration to the formation of cracks and in the end to a complete mechanical destruction [1]. In particular this applies to mineral building materials with low tensile strength such as sandstone. The consolidation of deteriorated sandstone by stone strengthener is aimed at regaining the original state with respect to strength and porosity [2] and to a certain degree to produce stress transfer over existing cracks.

The aim of the presented investigations was, to achieve from results of bending tests on sandstone a possible fracture

mechanical description and further to check the effect of cementation by a stone strengthener with respect to the cementation of cracks and the development stress transfer over cracks.

The modeling of failure processes in natural stone is based on a continuum mechanical description, wherein the assumption of a local tensile strength β as the only critical parameter is not sufficient. The reason for, is that the tensile strength, defined as quotient from fracture load and fracture area, has a significant dependence on the size of the test specimen. By tensile strength it's possible, to analyze whether a state of stress in a component part is permissible or not. But stress transfer resulting from crack formation is not considered. Furthermore it makes no sense to analyze the strength of component parts containing cracks, because there are theoretical predicted stress singularities at the crack tip [3].

Therefore the description of failure processes has to make use of fracture mechanics. The surface energy is an important material parameter, that can be determined from loading test. Furthermore the crack length in dependence of the applied load must be known. For the experimental determination of crack lengths and for the visualization of crack progress the holographic interferometry and image processing is a very useful tool because of its high range of sensitivity and the possibility of extensive observation [4].

2. Theory

During the crack formation and crack growth elastic energy is converted to surface energy. The amount of energy necessary for the generation of a crack surface is called the the specific fracture energy G_f .

In linear elastic fracture mechanics (LEFM) it is assumed, that the crack surfaces are unstressed -there is no transfer of tension stress. As a result of this, a stress singularity exists in the vicinity of the crack tip. The singularity is described by the stress intensity factor K_I [3]:

$$K_I = \sigma \cdot (a)^{1/2} \cdot f(a/d, b/a, \dots) \quad [\text{N/mm}^{3/2}] \quad (1)$$

σ : stress by external load in the uncracked specimen

a : crack length

f : nondimensional function

d, b, \dots : characteristic dimensions of the specimen

The energy balance due to the crack development can be stated as:

$$1/E \cdot K_I^2 = G_f \quad (2)$$

E : Young's modulus of elasticity

However, when the fracture energy G_f was evaluated from notched samples of mineral building material, a strong size dependence of G_f has been observed [5]. This size effect is attributed to nonlinear slow crack growth occurring prior the peak load; with increasing load a stable growth of the crack is obtained.

The modeling of this behaviour in the nonlinear fracture mechanics is based on the assumption, that the so called cohesive or crack-processing-zone exists, where stress transfer depending on the crack opening w is possible [6]. The fracture energy $G(w)$ is assumed to be a material typical function. The tensile strength β_z as well as the total fracture energy G_f necessary for the generation of an unstressed crack, can be deduced from $G(w)$. A simple possible

approach for $G(w)$ is the following equation [7]:

$$G(w) = G_f \cdot \{1 - \exp[-w \cdot \beta_z / G_f]\} \quad (3)$$

Considering the nonlinear dependence of the fracture energy from the crack opening the energy balance during crack progression can be stated as in equation (4):

$$1/E \cdot K_I^2(a) da = \int_0^{a+da} G[w(x, a+da)] dx - \int_0^a G[w(x, a)] dx \quad (4)$$

The LEFM as limiting case can be obtained from equat. (4) by setting $\beta_z \rightarrow \infty$. While the material property G_f can be evaluated from a load deflection diagram, however, the tensile strength has to be determined indirectly by comparison of experimental and calculated maximum loads. This follows from the fact, that the stress distribution ad hoc is unknown due to undercritical crack growth prior the ultimate load.

3. Test setup

Three different kinds of sandstone were used in the investigations: four samples consisting of Schilfsandstein from Schloß Schillingsfürst, three samples consisting of freshly-broken Rütthener Grünsandstein and four samples consisting of Stubensandstein from St.Vitus (Ellwangen). The original building material samples were prepared from a block from a depth of 50mm below the outer surface of the building.

In a first step notched beams of the dimensions 200mm·40mm·45mm were tested in a three-point bending arrangement. The notch length and the support span were 15mm and 180mm respectively. The test run was deformation controlled

and was finished, when the crack reached a length of 80% in relation to the crack ligament. During the test run, the external load and the centre deflection were measured. Real-time holographic interferometry was used for contact free crack detection and for the determination of crack lengths. Employing image processing the interference phase, that is improved in contrast and signal to noise ratio, can be evaluated from four phase-shifted interferograms. Cracks are detected from lines of unsteadiness either in the interferogram (fig.1) or the interference phase (fig.2)

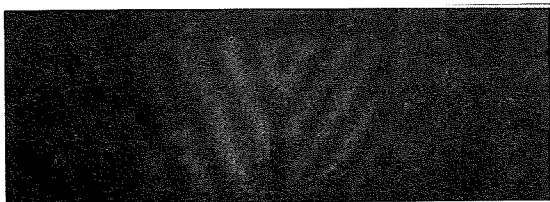


Fig.1 Interferogram of a loaded specimen

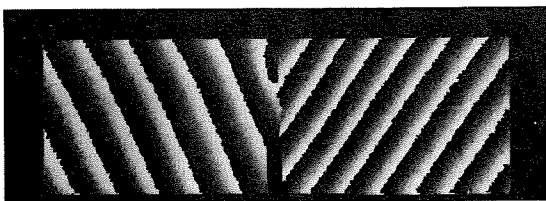


Fig.2 Interference phase modulo 2π

The test specimen containing cracks of a defined length were cemented using a stone strengthener on the basis of silicic acid ethyl ester. Submerging the samples for six times (until a saturation was reached) should correspond to a maximum strengthening. The total increase in weight during the consolidation was on average 4,6% at Schilfsandstein, 6,6% at

Grünsandstein and 2,4 % at Stubensandstein. From a second bending test on the consolidated samples the load-deflection curves as well as the crack growth versus external load was determined.

4. Experimental results

4.1 Load-deflection diagrams

In the following fig.'s 3-5 the experimental load-deflection diagrams of the untreated (a) and the strengthened (b) samples are given together with the result of a theoretical calculation (c). Since the variation within one kind of sandstone was small, only one diagram is presented as representative for the whole set.

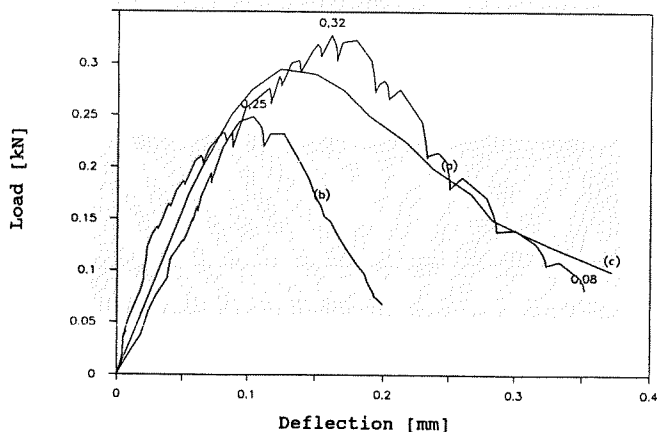


Fig.3 Load-deflection curves of Schilfsandstein
 (a) 1.loading of the untreated specimen
 (b) after cementation
 (c) theoretical prediction
 ($\beta_x = 2,5 \text{ N/mm}^2$, $G_f = 0,06 \text{ N/mm}$, $E = 2500 \text{ N/mm}^2$)

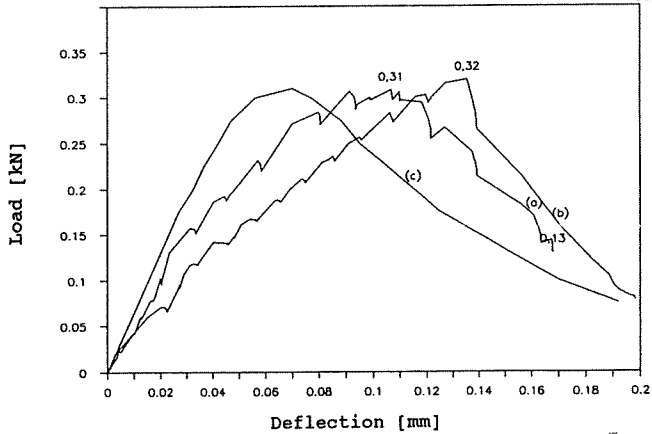


Fig.4 Load-deflection curves of Grünsandstein
 (a) 1.loading of the untreated specimen
 (b) after cementation
 (c) theoretical prediction
 ($\beta_z=3\text{N/mm}^2$, $G_z=0,03\text{N/mm}$, $E=5000\text{N/mm}^2$)

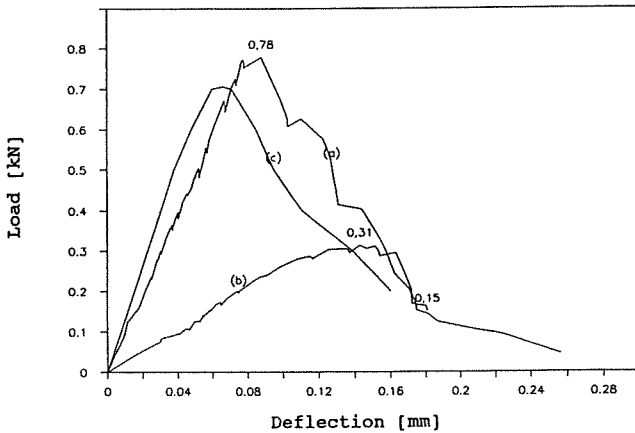


Fig.5 Load-deflection curves of Stubensandstein
 (a) 1.loading of the untreated specimen
 (b) after cementation
 (c) theoretical prediction
 ($\beta_z=10\text{N/mm}^2$, $G_z=0,06\text{N/mm}$, $E=10000\text{N/mm}^2$)

In table 1 the mean values of the maximum load, the load at the end of the first bending test and the fracture energy G_f are listed. The crack mouth opening at the end of the first loading can be estimated to be 0,1-0,01mm.

	Schilf-sandstein	Grün-sandstein	Stuben-sandstein
peak load [kN] first loading	0,30	0,34	0,73
end load [kN] first loading	0,10	0,15	0,15
peak load [kN] after cementation	0,25	0,33	0,29
G_f [N/mm] first loading	0,061	0,029	0,060
G_f [N/mm] after cementation	0,029	0,028	0,030

Tab.1

The mean value of the peak load at the first loading is for Stubensandstein considerably higher than these for Schilfsandstein and Grünsandstein. However, the peak loads of all strengthened samples are approximately equal. The fracture energy at the first loading of Grünsandstein is approximately half the value of Schilfsandstein and Stubensandstein. All the strengthened specimens show a uniform deformation and fracture behaviour and equal values of the fracture energy. That leads to the conclusion, that the deformation behaviour of the strengthened specimen is depending essentially on the properties of the stone strengthener and less on the mechanical properties of the stone.

4.2 Crack growth

The crack growth versus the external load, which was evaluated from the interferograms, is plotted in the fig.6-8 for the investigated kinds of sandstone. As in 4.1 the curves of one sample at first loading and after strengthening are shown.

With all samples crack formation prior the peak could be observed. The crack length at maximum load was approximately 20-30% related to the crack ligament. Therefore the investigated stones show a nonlinear fracture behaviour, that is predicted from the existence of a crack-processing zone.

From the crack-growth diagrams of the strengthened samples it is obvious, that the crack as a result of the first loading is opens completely at rather small loads. In comparison to the untreated samples however, the maximum load is reached at considerably high crack lengths. This fact leads

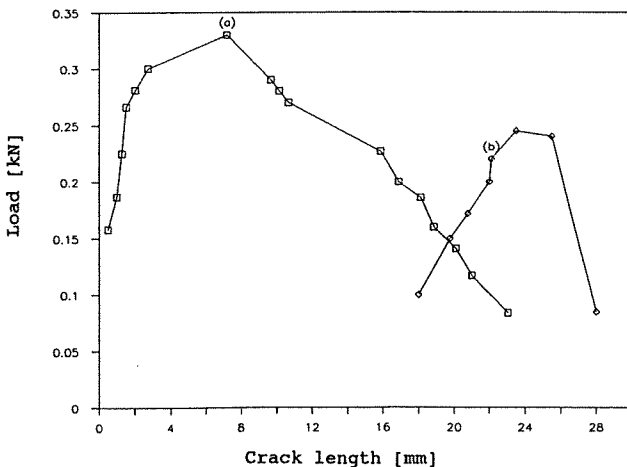


Fig.6 Schilfsandstein, crack growth
(a) 1.loading of the untreated specimen
(b) after cementation

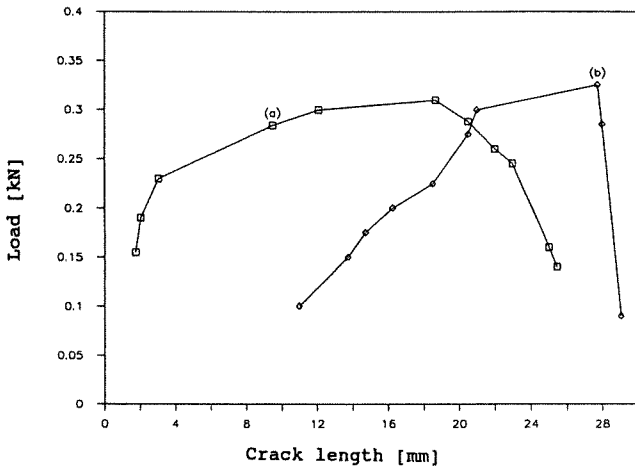


Fig.7 Grünsandstein, crack growth
 (a) 1.loading of the untreated specimen
 (b) after cementation

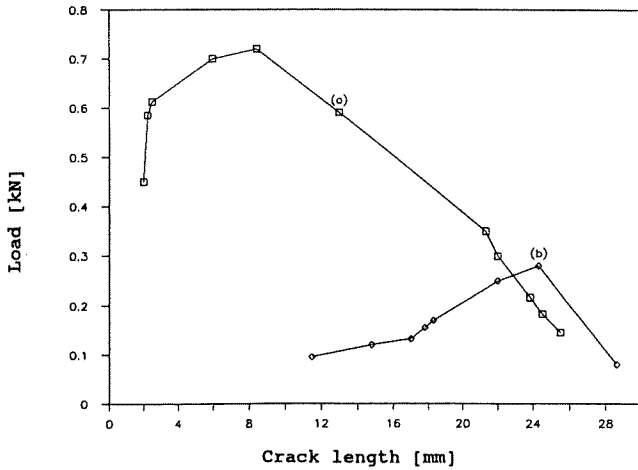


Fig.8 Stubensandstein, crack growth
 (a) 1.loading of the untreated specimen
 (b) after cementation

to the conclusion, that the stress transfer over the crack is increased as a result of the strengthening. Obviously an effective stress transfer is only possible at large deformations, corresponding to the nonlinear stress-strain characteristic of rubber-like material. Thus the effect of the strengthening is not the complete cementation of cracks, but the improvement of stress transfer over the crack at large deformations.

4.3 The fracture mechanical model, conclusions

From undercritical crack growth occurring at the loading of the untreated samples, it can be concluded, that a nonlinear crack-zone exists. The calculated load-deflection diagrams considering nonlinear effects correspond well to experimental results (fig's.3-5).

The stress intensity factor K_I (fig.8-11), that was calculated from experimental data, shows a significant dependence on the crack length. Therefore it is obvious, that the fracture behaviour of the investigated sandstones can only be explained by nonlinear crack-zone effects.

	Schilf-sandstein	Grün-sandstein	Stuben-sandstein
K_I [N/mm ^{1,5}] at maximum load first loading	12	16	36
K_I [N/mm ^{1,5}] at maximum load after cement.	64	130	145

Tab.2

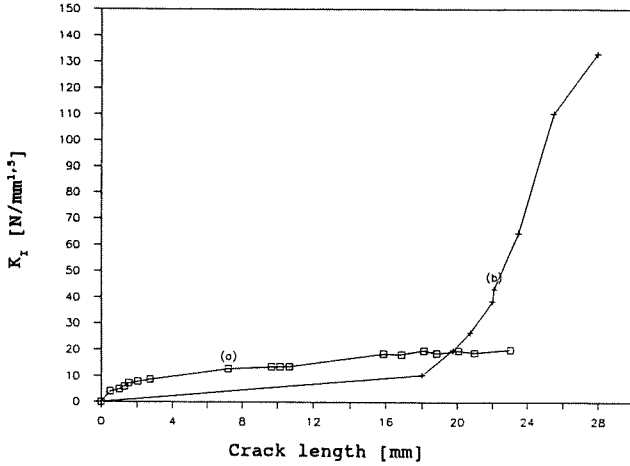


Fig.9 Schilfsandstein, stress intensity factor versus crack length
 (a) 1.loading of the untreated specimen
 (b) after cementation

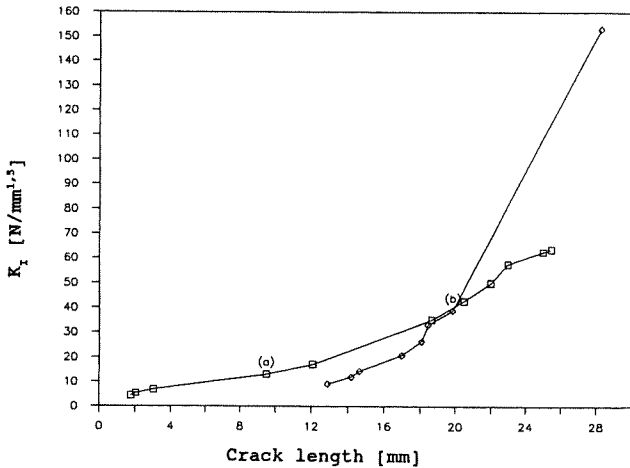


Fig.10 Grünsandstein, stress intensity factor versus crack length
 (a) 1.loading of the untreated specimen
 (b) after cementation

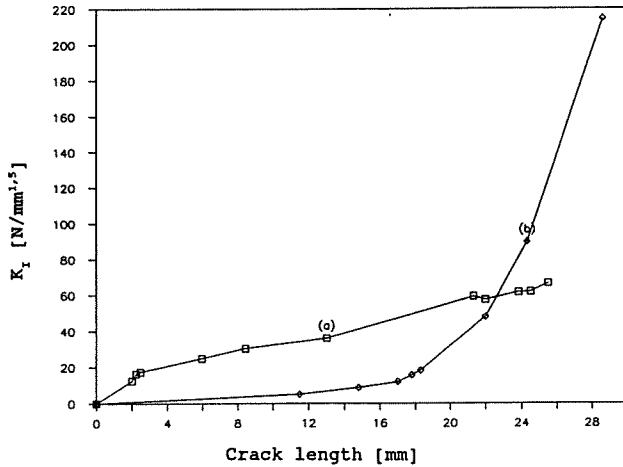


Fig.11 Stubensandstein, stress intensity factor versus crack length
 (a) 1. loading of the untreated specimen
 (b) after cementation

Furthermore the fracture behaviour is affected by time-dependent effects. This is indicated by the quasi-viscous deflection behaviour.

The strengthening leads to an increase of stress transfer over cracks. This is shown clearly by the fig's.8-11 and table 2, where the values of the stress intensity factor after the strengthening considerably exceed the values than during the first loading.

5. References

- [1] Schuh, H.: Physikalische Eigenschaften von Sandsteinen und ihren verwitterten Oberflächen; Münchner Geowissenschaftliche Abhandlungen; Verlag Friedrich Pfeil (1987)
- [2] Snethlage, R.: Steinkonservierung; Forschungsprogramm des Zentrallabors für Denkmalpflege 1979-1983; Arbeitsheft 22; Hrsg.: Bayrisches Landesamt für Denkmalpflege
- [3] Sähn, S.; Göldner, H.: Bruch- und Beurteilungskriterien in der Festigkeitslehre; Leipzig (1989)
- [4] Erf, R.: Holographic Nondestructive Testing; Academic Press, New York (1974)
- [5] Jenq, Y.S.; Shah, S.P.: A two Parameter Model for Concrete; J. of Engineering Mechanics, ASCE 111 No.10 (1985)
- [6] Hillerborg, A.: Analysis of One Single Crack Developments, Fracture Mechanics of Concrete, Elsevier (1983)
- [7] Eligehausen, R.; Sawade, G.: Verhalten von Beton auf Zug; Beton+Fertigteilewerk-Technik, Heft 7/8 (1985)